HHS Public Access

Author manuscript

*J Allergy Clin Immunol*. Author manuscript; available in PMC 2020 June 01.

Published in final edited form as:

*J Allergy Clin Immunol*. 2019 June ; 143(6): 2215–2226.e7. doi:10.1016/j.jaci.2018.10.068.

# IFN-γ and CD25 drive distinct pathological features during hemophagocytic lymphohistiocytosis

**Stéphanie Humblet-Baron, MD PhD**[1,2,*], **Dean Franckaert, PhD**[1,2,*], **James Dooley, PhD**[1,2], **Fatima Ailal, MD**[3], **Aziz Bousfiha, MD**[3], **Caroline Deswarte, MSc**[4,5], **Carmen Oleaga-Quintas, MSc**[4,5], **Jean-Laurent Casanova, MD PhD**[4,5,6,7,8], **Jacinta Bustamante, MD PhD**[4,5,6,9], **Adrian Liston, PhD**[1,2,^]

[1]VIB Center for Brain & Disease Research, Leuven 3000, Belgium, EU

[2]KU Leuven - University of Leuven, Department of Microbiology and Immunology, Leuven, Belgium, EU

[3]Clinical Immunology Unit, Casablanca Children's Hospital, Ibn Rochd Medical School, King Hassan II University, Casablanca, Morocco

[4]Laboratory of Human Genetics of Infectious Diseases, Necker Branch, INSERM U1163, Imagine Institute, Necker Hospital for Sick Children, Paris, France

[5]Paris Descartes University, Paris, France, EU

[6]St. Giles Laboratory of Human Genetics of Infectious Diseases, Rockefeller Branch, The Rockefeller University, NY, USA

[7]Howard Hughes Medical Institute, NY, USA

[8]Pediatric Hematology-Immunology Unit, Assistance Publique-Hôpitaux de Paris AP-HP, Necker Hospital for Sick Children, Paris, France, EU

[9]Center for the Study of Primary Immunodeficiencies, Assistance Publique-Hôpitaux de Paris AP-HP, Necker Hospital for Sick Children, Paris, France, EU

## Abstract

**Background—**The inflammatory activation of $CD8^+$ T cells can, when unchecked, drive severe immunopathology. Hyper-stimulation of $CD8^+$ T cells, through a broad set of triggering signals,

^ correspondence to adrian.liston@vib.be. **Address for correspondence:** Adrian Liston; Autoimmune Genetics Laboratory, VIB, Leuven, Belgium, and the Department of Microbiology and Immunology, University of Leuven, Herestraat 49, 3000 Leuven, Belgium. Tel + 32 163 30934; Fax +32 163 0591 adrian.liston@gmail.com.

*Equal contribution first authors

AUTHOR CONTRIBUTIONS

DF, SHB and JD performed the experiments and analyzed the data. SHB and AL designed the experiments. DF, SHB and AL wrote the manuscript. FA, AAB, CD, JB and JLC provided all the patient data and contributed to writing the manuscript. All authors commented on and discussed the paper.

CONFLICTS OF INTEREST DISCLOSURES

The authors declare no conflicts of interest.

can precipitate hemophagocytic lymphohistiocytosis (HLH), a life-threatening systemic inflammatory disorder.

**Objective—**The mechanism linking $CD8^+$ T cell hyper-activation to pathology is controversial, with excessive production of IFN-γ and, more recently, excessive consumption of IL-2, proposed as competing hypotheses. We formally tested the proximal mechanistic events of each pathway in a mouse model of HLH.

**Methods—**In addition to reporting a complete IFN-γR1 deficient patient with multiple aspects of HLH pathology, we used the mouse model of $Prf1^{KO}$ mice infected with LCMV to genetically eliminate either IFN-γ production or CD25 expression and assess the immunological, hematological and physiological disease measurement.

**Results—**We found a striking dichotomy between mechanistic basis of the hematological and inflammatory components of $CD8^+$ T cell-mediated pathology. The hematological features of HLH were completely dependent on IFN-γ production, with complete correction following loss of IFN-γ production, without any role for $CD8^+$ T cell-mediated IL-2 consumption. The mechanistic contribution of the immunological features, by contrast, were reversed, with no role for IFN-γ production, but substantial correction following the reduction of IL-2 consumption by hyper-activated $CD8^+$ T cells. These results were complemented by the characterization of an IFN-γR1-deficient HLH-like patient, where multiple aspects of HLH pathology was observed in the absence of IFN-γ signaling.

**Conclusion—**These results synthesize the competing mechanistic models of HLH pathology into a dichotomous pathogenesis driven through discrete pathways. A holistic model provides a new paradigm for understanding HLH, and, more broadly, the consequences of $CD8^+$ T cell hyper-activation, thereby paving the way for clinical intervention based on the features of HLH in individual patients.

## Capsule summary

Studying the pathogenesis of hemophagocytic lymphohistiocyosis, we found a striking dichotomy between the hematological and inflammatory components of HLH. Hematological features are strictly dependent of IFN-γ, while inflammation is driven by dysregulated IL-2 signaling.

## Graphical Abstract

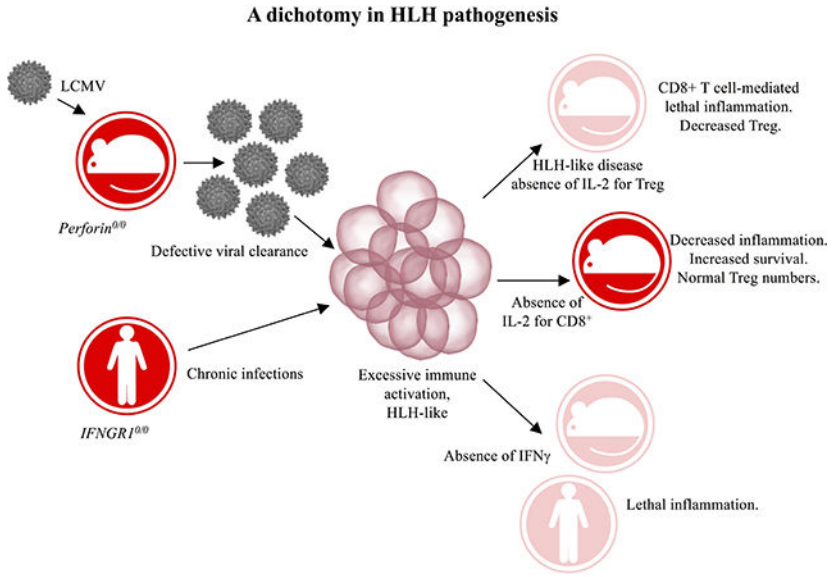


**Keywords**

IFN-γ; CD25; CD8+ T cell hyper-activation and hemophagocytic lymphohistiocytosis

## INTRODUCTION

Hemophagocytic lymphohistiocytosis (HLH) is a life-threatening systemic inflammatory disorder. The inflammation in this disease is characterized by an excessive activation of the immune system (mainly cytotoxic T cells and macrophages) and a cytokine storm (including IFN-γ, IL-6 and TNF-α). Clinical manifestations include prolonged fever, cytopenia, hepatosplenomegaly, hepatitis, and, in some patients, neurological symptoms. Classical presentation can lead to patient death by uncontrolled inflammation, multiple organ failure or secondary severe infection, if left untreated [1–3]. Successful treatment requires drastic clinical intervention through steroids, etoposide and immunosuppressive reagents, with only a 50 to 60% survival rate [4–6].

HLH is a broad clinical term, encompassing a diverse set of inflammatory contexts mediated by $CD8^+$ T cell hyper-activation. Primary HLH refers to patients with severe inherited defects in genes related to the cytotoxic pathways of T and NK cells, or in genes involved in Epstein Barr virus (EBV) clearance, with viral infection frequently serving as a trigger for clinical manifestation [7]. When a genetic cause is established, allogeneic hematopoietic stem cell transplantation (allo-HSCT) is the only curative treatment. Secondary or acquired HLH encompasses patients who develop the syndrome as a consequence of escalating $CD8^+$ T cell responses against infections (mainly after EBV and cytomegalovirus (CMV), but also after bacterial, fungal or parasitic infections), malignancies (mainly lymphomas) or autoimmune targets, such as occurs in systemic juvenile idiopathic arthritis or systemic lupus erythematosus [1,3,5,8]. HLH thus serves as the archetype for understanding the pathology mediated by hyper-activation of $CD8^+$ T cells within a general clinical context. The poor prognosis of HLH patients, even when given the best current treatments, indicates

that our understanding of the molecular basis of this disease is unsatisfactory. HLH is a complex disease comprising two main features with both immunological manifestations, including cytotoxic T cell activation and cytokine storm, and hematological manifestations, with severe anemia. In addition, hemophagocytosis describes the presence of activated macrophages able to engulf blood cells, and its presence has been reported to be a direct contributor to anemia [9]. Whether the immunological and hematological aspects of the disease share a common mechanistic basis, or independently arise from distinct molecular mechanisms has not been explored to date.

One of the key developments in the understanding of HLH has been the development of a mouse model that recapitulates the key features of patients. The mouse model utilizes *Perforin*$^{KO}$ mice (*Prf1*$^{KO}$), replicating the common *PRF1* mutation in primary HLH. *Prf1*$^{KO}$ mice are healthy in the baseline state, however when infected with lymphocytic choriomeningitis virus (LCMV), *Prf1*$^{KO}$ mice develop many of the same hematological and immunological characteristics of HLH, with severe anemia and fatal inflammation [10,11]. Analysis of HLH patients and the HLH mouse model has been used to develop a working model for HLH pathogenesis. In this model, defects in cytotoxicity result in higher viral titers and an inability to clear antigen presentation cells, leading to extended immune stimulation and increased activation of CD8$^+$ T cells [12]. These CD8$^+$ T cells then have amplified expression of cytokines which further precipitate systemic inflammation including the activation of other immune cells, especially macrophages, creating a cytokine storm [11]. IFN-γ is thought to be the most critical cytokine in HLH pathology, with both the hematological and inflammatory aspects of the disease attributed to its excessive production [9,11,13,14]. The role of IFN-γ has, however, been recently challenged, with the findings of HLH in patients with genetic defects in the IFN-γ pathway [15–17]. Specifically, three patients have been reported with HLH disease and an IFN-γR defect, although among these only one patient received a definitive diagnostic of a complete absence of IFN-γ signaling through IFN-γR2, while the other two patients had either a partial defect or an implied defect of IFN-γR1[15,16]. Supporting the IFN-γ-independence of disease, development of a systemic juvenile idiopathic arthritis-like inflammation has been described in *IFN-γ* knockout mice [18,19]. And finally, gene expression profiling of peripheral blood mononuclear cells (PBMC) from children with untreated HLH failed to identify differential expression of IFN-γ or IFN-γ regulated genes as an HLH signature [20]. We recently proposed an additional alternative model of HLH pathogenesis [21]. CD8$^+$ T cells from LCMV-infected *Prf1*$^{KO}$ mice not only exhibit hyper-production of IFN-γ, but also manifest extreme expression level of the IL-2 receptor alpha (CD25). The enhanced consumption of IL-2 by activated CD8$^+$ T cells is accompanied by a collapse in regulatory T cell (Treg) numbers [21], a feature which could account for the feed-forward inflammatory loop observed in HLH patients. While these models are not mutually exclusive, resolution of this controversy is of great importance as a clinical trial using anti-IFN-γ antibody in HLH patients is currently ongoing [22].

Here we sought to formally test the competing hypotheses for the pathological mechanisms of CD8$^+$ T cell hyper-stimulation in HLH. In addition to reporting a complete IFN-γR1 deficient patient with multiple aspects of HLH pathology, we used the mouse model of *Prf1*$^{KO}$ mice infected with LCMV to genetically eliminate either IFN-γ production or CD25 expression and assess the immunological, hematological and physiological disease

measurement. We found a striking dichotomy between the hematological and inflammatory components of HLH pathology. IFN-γ production during HLH was essential for the hematological features, with the loss of IFN-γ completely correcting anemia, but having no effect on immune activation, wasting and survival. By contrast, restricting IL-2 consumption by $CD8^+$ T cells had no impact on the hematological features of HLH, but restored Treg numbers, suppressed the hyper-inflammatory state and extended the life-span. These results provide a paradigm shift for the understanding of the consequences of $CD8^+$ T cell hyper-activation, with the two sets of symptoms (inflammatory and hematological) driven through dichotomous pathways, which together drive the HLH clinical presentation.

## MATERIALS AND METHODS

### Patient

Clinical data were obtained from the patient developing HLH symptoms during clinical care in Casablanca, Morocco. Further diagnostic investigation was performed at the Laboratory of Human Genetics of Infectious Diseases, INSERM U1163, Imagine Institute, in accordance with local regulations, and with the approval of the IRB of Necker Hospital for Sick Children, Paris, France. Written informed consent was obtained by the patient family.

### Mice

Perforin-deficient (C57BL/6-*Prf1*$^{tm1Sdz}$/J) [23], IFN-γ-deficient (C57BL/6-*Ifng*$^{tm1Ts}$) [24] and CD8-Cre transgenic mice (C57BL/6-Tg(Cd8a-cre)1Itan/J) [25] were obtained from The Jackson Laboratory (Bar Harbor, ME) and were used on the C57BL/6 background. *CD25*$^{KO}$ mice were generated from EUCOMM embryonic stem cells, with production through blastocyst injection. Transgenic founders were transiently intercrossed with Flpase mice (FLPe) [26], to excise the neomycin resistance cassette and convert the allele to a floxed status. The resulting *CD25*$^{fl/fl}$ mice were backcrossed to the C57BL/6 background >8 generations prior to intercross with CD8-Cre mice. All mice were maintained in specific pathogen-free facilities of University of Leuven. All experiments were approved by the University of Leuven Animal Ethics Committee. All mice were used at 8–15 weeks of age.

### Virus and infection

LCMV-Armstrong was produced and titrated as previously described [27]. Briefly, The LCMV strain was propagated in baby hamster kidney cells and titrated on Vero African green monkey kidney cells as previously described [28].At 8–12 weeks of age, mice were infected with $10^5$ PFU of LCMV-Armstrong intraperitoneally (day 0) and were monitored and analyzed at day 10 post-infection for immunological and hematological parameters.

### Blood and plasma analysis

Mouse blood samples were analyzed on Cell-Dyn 3700 (Abbott) to determine red blood cell and platelet counts as well as hematocrit and hemoglobin contents. Plasma samples were analyzed determined by a mouse IL-2Rα DuoSet ELISA (R&D System) and the MSD inflammatory cytokine panel according the manufacturers' protocol.

### Genomic DNA and whole exome-sequencing (WES)

Genomic DNA was extracted from whole blood and 3μg was sent for WES. Briefly, an adapter-ligated library was prepared with the Paired-End Genomic DNA Sample Prep kit V1 (Illumina). The SureSelect Human All Exon kit (Agilent Technologies) was then used for exome capture. Exome capture was performed with the 71Mb SureSelect Human All Exon kit (Agilent Technologies).

### In vitro patient cell line analysis

EBV-transformed B lymphocytes (EBV-B cells) were generated from freshly collected PBMCs. IFN-γR1 expression (phycoerythrin PE labeled mAbs specific human or isotype-matched controls from BD Biosciences) on the surface of EBV-B cells were performed by flow cytometry analysis as previously described [29]. EBV-B cells were stimulated for 30 minutes with IFN-γ ($10^5$ IU/ml) or IFN-α ($10^5$ IU/ml) and phospho-STAT1 (anti-Y701-pSTAT1-Alexa468, 612132, BD Transduction laboratory) was detected by flow cytometry analysis. Staining was assessed on a Galios cytometer (Beckman Coulter), and the results were analyzed with FlowJo v10.

### Mutation testing

The wild-type *IFNGR1* allele was inserted into V5-topo-pcDNA3.1 (Invitrogen). The p.W99R and c.131del mutants were generated by site-directed mutagenesis (Agilent Technologies, PfuUltra II Fusion HS DNA polymerase). IFN-γR1-deficient SV40-fibroblasts were transfected with an insert-less V5-tagged pcDNA3.1 plasmid (Empty Plasmid, EV) and one of the *IFNGR1* V5-tagged pcDNA3.1 plasmids in the presence of X-treme GENE9 transfection reagent (Sigma Aldrich). Total proteins were solubilized in extraction buffer as previously described [30]. Samples were run on SDS-PAGE in 10% polyacrylamide gels (Bio-Rad), and the resulting bands were transferred onto fluorescence PVDF membranes (Bio-Rad) with the Trans-Blot Turbo Transfer System (Bio-Rad). Immunoblotting was performed with antibodies against GAPDH (14C10, Cell Signaling Technology) and the V5 tag (Thermo Fisher Scientific). Bound antibody was detected with ECL western blotting detection reagents (Bio-Rad) on Chemidoc. Electrophoretic mobility shift assay (EMSA) was carried out as previously described [30]. Briefly, cells were stimulated for 20 minutes with IFN-γ at $10^4$ IU/ml. We then obtained a nuclear extract from these cells, and incubated 5–10 μg of this nuclear extract with IRDye 700 gamma-activating sequence (GAS) probe, corresponding to the Fc-γR1 promoter, subjected the mixture to electrophoresis in a polyacrylamide gel and read with LI-COR Clx machine.

### Degranulation assay

Degranulation of human NK cells and $CD8^+$ T cells were performed as following; $3\times10^5$ PBMC were incubated for 3 hours *in vitro* alone, in presence of 1:1 K562 cells, or with phorbol 12-myristate 13-acetate (50 ng/mL; Sigma-Aldrich), and Ionomycin (250 ng/mL; Sigma-Aldrich). Cells were then stained for surface staining including CD3 (SK7), CD8 (RPA-T8), CD56 (MEM188), CD16 (CB16), CD107a (LAMP-1) and CD107b (H4B4) (all from Invitrogen, Thermofisher) and CD14 (M5E2, from Biolegend) and analyzed by flow cytometer CANTO II (BD Bioscience).

### Histology

Tissues were fixed in 4% PFA and continued to trimming and processing for hematoxylin and eosin staining. Images were evaluated on a Nikon Labophot-2 microscope and captured using a Nikon D5000 digital microscopic camera. Histopathological analysis was performed blinded and subjectively by BioGenetics Research Laboratories (WA, USA) as before [31,32]. Briefly, severity score 1 was used to include pathological findings that showed no significant lesions and normal morphology. Severity score 2 was assigned to all tissues showing minimal (minor and infrequent, <10% of defined area) and mild (noticeable microscopic change but no overt feature, 11–20% of defined area involved in case of focal, multifocal or diffuse effects). Moderate findings including prominent changes (21–40% of defined area for focal, multifocal or diffuse effects) were assigned severity score 3. Overwhelming microscopic features (41–100% for focal, multifocal or diffuse effects in defined area) were assigned severity grade 4.

### Flow cytometry

Single-cell suspensions were prepared from mouse spleen and pooled lymph nodes (cervical, inguinal, mesenteric, axillary and brachial). For intracellular cytokine staining, lymphocytes were plated at $5\times10^5$ cells/well in 96 well tissue culture plates in complete RPMI containing phorbol myristate acetate (50 ng/mL; Sigma-Aldrich), ionomycin (250 ng/mL; Sigma-Aldrich) and monensin (1/1500; BD, Bioscience) for 4 hours at 37°C. All cells were fixed with BD Cytofix™ (BD, Biosciences) or fixed and permeabilized with the eBioscience Foxp3 staining kit (eBioscience). Anti-murine antibodies included anti-CD4 (RM4–5), anti-CD8a (53–6.7), anti-FoxP3 (FJK-16s), anti-CD25 (PC61.5), anti-CD127 (A7R34), anti-CTLA4 (UC10–4B9), anti-CD69 (H1.2F3), anti-CD103 (2E7), anti-CD44 (IM7), anti-CD62L (MEL-14), anti-IL-2 (JES6–5H4), anti-IFNγ (XMG1.2), anti-KLRG1 (2F1), anti-PD1 (J43 and anti-phospho-STAT5 (SRBCZX) and anti-Ki67 (SolA15) from eBioscience. Data were collected on BD CANTO II (BD Biosciences) and analyzed using FlowJo for Mac version 9.6 (Tree Star Inc.).

### Statistics

Statistical analysis was performed with a one-way ANOVA with Tuckey's multiple comparisons test. All statistical analyses were carried out with GraphPad Prism (version 7; GraphPad Software, La Jolla, Calif).

## RESULTS

### IFN-γ production drives the hematological, but not immunological, components of HLH pathology

LCMV infection of *Prf1*$^{KO}$ mice constitutes a robust mouse model of HLH, with hematological abnormalities, exuberant inflammation and early mortality [11]. Previous studies using genetic deficiency or antibody-mediated neutralization have highlighted the role of IFN-γ in the anemia occurring in LCMV-infected *Prf1*$^{KO}$ mice [9,11,13,14], however the other aspects of HLH pathology have not been assessed. We backcrossed *Prf1*$^{KO}$ mice with *IFN-γ*$^{KO}$, creating *Prf1*$^{KO}$ *IFN-γ*$^{KO}$ double knockout (DKO) mice. LCMV infection of

wildtype, *Prf1*$^{KO}$ mice and *Prf1*$^{KO}$ *IFN-γ*$^{KO}$ DKO mice produced a severe disruption of the erythroid cell compartment in *Prf1*$^{KO}$ mice which was completely corrected in DKO mice (Figure 1A–C). *IFN-γ*$^{KO}$ mice, with wildtype perforin, did not exhibit any hematological abnormalities (Figure 1A–C). Intriguingly, while the anemia was prevented by IFN-γ-deficiency, DKO mice still exhibited liver hemophagocytosis (Figure 1D, E). This data demonstrates that low red cell counts, hemoglobin and hematocrit are IFN-γ-dependent pathologies.

Having established the IFN-γ-dependency of the hematological signature of HLH, we next assessed the physiological and immunological components of the disease. Unlike wildtype mice, *Prf1*$^{KO}$ mice present with distressed behavior during the late stages of LCMV infection, coupled with severe wasting necessitating euthanasia at day 10 (Figure 2A). Despite a complete recovery of hematological abnormalities, *Prf1*$^{KO}$ *IFN-γ*$^{K}$ DKO mice developed the same distressed behavior and wasting, also requiring euthanasia at day 10 (Figure 2A). *Prf1*$^{KO}$ mice demonstrated an enlarged spleen and liver damage after LCMV infection, which was also unaffected IFN-γ genotype (Supplementary Figure 1). In HLH, one of the primary pathological events is the infiltration and destruction of tissues, leading to multiple organ failure [3,5]. While wildtype and *IFNγ*$^{KO}$ recovered from LCMV infection without widespread liver damage, *Prf1*$^{KO}$ and *Prf1*$^{KO}$ *IFN-γ*$^{KO}$ DKO both experienced extensive reticuloendothelial cell infiltration (Figure 2B). The physiological manifestations of HLH pathology were therefore not dependent on excessive IFN-γ production.

Previous publications from our group and others have previously demonstrated a clear correlation between serious weight loss and critical inflammation in mouse HLH model [21,33]. Therefore, we performed a detailed scrutiny of the immune compartment. First, CD8$^{+}$ T cells, which are known to be responsible for the disease severity [11], were elevated in the lymph nodes of *Prf1*$^{KO}$ *IFN-γ*$^{KO}$ DKO mice to an even greater degree than *Prf1*$^{KO}$ mice (Figure 2C). In *Prf1*$^{KO}$ mice infected with LCMV, there is not only an increase in the size of the CD8$^{+}$ T cell compartment, but also a marked shift towards an activated phenotype, with high percentages of effector memory subsets (CD8$^{+}$CD44$^{+}$CD62L$^{-}$) and short-lived effector cells (SLEC; CD8$^{+}$CD44$^{+}$KLRG1$^{+}$CD127$^{-}$) which are both hallmarks of HLH inflammatory condition (Figure 2D). *Prf1*$^{KO}$ *IFN-γ*$^{KO}$ DKO mice, despite the absence of IFN-γ, exhibited the same escalation of these inflammatory mediators as *Prf1*$^{KO}$ mice, well above the levels normally associated with LCMV infection in wildtype or *IFN-γ*$^{KO}$ mice (Figure 2D). We recently added exuberant CD25 expression on CD8$^{+}$ T cells to the characteristic hallmarks of murine HLH, a condition associated with Treg collapse [21]. This immunological manifestation was reproduced here in *Prf1*$^{KO}$ mice, with an identical presentation in *Prf1*$^{KO}$ *IFN-γ*$^{KO}$ DKO mice. Specifically, CD25 expression as both a percentage (Figure 2E) and intensity (Figure 2F) were higher on CD8$^{+}$ T cells from LCMV-infected *Prf1*$^{KO}$ and *Prf1*$^{KO}$ *IFN-γ*$^{KO}$ DKO mice than the LCMV-infected wildtype or *IFN-γ*$^{KO}$ controls. Moreover, high levels of soluble CD25 (sCD25) in the serum has been used as a diagnostic marker for HLH [1,5], and when analyzed in our cohort, sCD25 was found at the highest level in *Prf1*$^{KO}$ and *Prf1*$^{KO}$ *IFN-γ*$^{KO}$ DKO mice, clearly emphasizing the presence of systemic inflammation (Figure 2G). Similar results were seen with CD4$^{+}$ T cells, with elevated activation in *Prf1*$^{KO}$ mice which was not ameliorated by the additional loss of IFN-γ (Supplementary Figure 2). These data clearly demonstrated that the immunological

features of HLH arise independent of the expression of IFN-γ, with hyper-activated $CD8^+$ T cells still possessing deleterious effects on normal mouse physiology.

## Development of HLH in a patient with an absence of IFN-γ signaling

We identified a patient affected by a complete IFN-γR1 deficiency that developed multiple HLH diagnostic criteria secondary to severe mycobacterial infection (Figure 3A). A 2 month old girl, from first degree consanguineous parents from Morocco, was diagnosed with BCG vaccine reactivation with presence of homolateral lymphadenopathy. There was no improvement despite antibiotherapy. Two months later, her clinical status further deteriorated and HLH diagnosis was made in presence of splenomegaly, high fever, pancytopenia (anemia and thrombocytopenia), hyperferritinemia and hypertriglyceridemia (Supplementary Table 1). While her blood showed normal level of NK cells (number and percentage according to the age of the patient), NK cell function was impaired (Supplementary Figure 3) and samples for sCD25 assessment were not available. Hemophagocytosis was not found in her bone marrow. The patient received antibiotics (ciproxin, amikacin, clarithromycin, rifampicin, isoniazid, ethambutol), steroids and cyclosporine and blood transfusions. The patient stabilized under this regime. Further clinical investigation of the patient was not possible. With a severe mycobacterial infection at a young age further investigation regarding the genetic origin of the disease was performed suspecting Mendelian susceptibility to mycobacterial disease (MSMD)[34]. A rare homozygote missense mutation, p.W99R, within *IFNGR1* gene was detected by WES. This mutation was confirmed by Sanger. Mother was heterozygous for this mutation. No DNA sample was available for father. No mutation in the genes involved in primary HLH was detected. (Figure 3B). While IFNGR1 protein was detected at a level comparable to healthy control (Figure 3C), further in vitro assay demonstrated a complete deficiency in the receptor signaling, with an absence of STAT1-Y701phosphorylation in the patient EBV-B cells after IFN-γ stimulation *in vitro*, while stimulation after IFN-α promoted normal STAT1 phosphorylation (Figure 3D). To formally characterize the *IFNGR1* allele we used an exogenous expression system. IFN-γR1-deficient primary human fibroblasts immortalized with SV-40T antigen (SV40-fibroblasts) were transiently transfected with wild-type (WT), p.W99R, and c.131del (defined loss of expression allele, responsible of complete AR IFNγR1 deficiency) IFNGR1 cDNA. As with the analysis of primary patient cells, the p.W99R allele in this transfection system demonstrated normal levels of protein expression (Figure 3E). Cells were stimulated with IFN-γ and gamma-activated factor-DNA binding activity was evaluated by EMSA using a GAS probe. SV-40 fibroblasts transfected with p.W99R had an abolished response to IFN-γ, similar to a negative control (Figure 3F). These findings demonstrate that the p.W99R allele is a loss of signaling function allele with normal protein expression. In the patient, a high level of IFN-γ on plasma, absence of IL-12p70 production (after BCG+ IFN-γ activation), normal IFN-γ production (after BCG+ IL-12p40 activation) in whole blood assay were also detected (data not shown), as found in other patients with complete IFN-γR1 deficiency[34]. Building upon previously reported HLH cases with impaired IFN-γ[15–17], this patient demonstrates that multiple aspects of HLH pathology can arise with a complete absence of IFN-γ signaling. Furthermore, the absence of hemophagocytosis in an IFN-γR1-deficient HLH-like patient complements the mouse

data (above), in that hematological aspects of HLH may be IFN-γ-dependent, even though overall disease progression was not.

## IL-2 consumption by hyper-activated CD8+ T cells contributes to the immunological and pathophysiological processes of HLH without altering the hematological features

In order to test the role of IL-2 consumption by $CD8^+$ T cells during hyper-stimulation, we generated $CD25^{flox}$ mice from EUCOMM ES cells (Supplementary Figure 4), deleted the lacZ and neo with a FLPe deleter strain [26] and intercrossed them with mice bearing the $CD8^+$ peripheral enhancer-driven Cre transgene [25]. The system preserves the expression of CD25 on Tregs, and allows $CD8^+$ T cells access to IL-2 consumption via the constitutively expressed low-affinity dimeric IL-2 receptor, but prevents the activation-induced expression of the high-affinity trimeric IL-2 receptor. The $CD8^{\Delta CD25}$ mice were then backcrossed to the $Prf1^{KO}$ background, allowing the comparison of wildtype, $Prf1^{KO}$ and $Prf1^{KO}CD8^{\Delta CD25}$ mice during LCMV-infection. The IL-2 consumption model is based on the observation that $CD8^+$ T cells from LCMV-infected $Prf1^{KO}$ mice express CD25 levels greater than those observed on Tregs, resulting in a rewiring of IL-2 consumption from Tregs to $CD8^+$ T cells and a collapse in Treg number [21]. We therefore first checked whether the $CD8^{\Delta CD25}$ strategy prevented rewiring of IL-2 consumption. Few $CD8^+$ T cells express CD25 in wildtype mice, even 10 days after LCMV infection (Figure 4A). $Prf1^{KO}$ mice, by contrast, show a dramatic increase, with CD25 expressed by >50% of CD8+ T cells. This increase was absent in $Prf1^{KO}CD8^{\Delta CD25}$ mice, which, akin to wildtype mice, showed no prominent $CD25^+$ population (Figure 4A). The effect of CD25 expression on IL-2 consumption (as measured through phosphorylation of STAT5) was dramatic: wildtype mice demonstrated no notable phosphoSTAT5 in $CD8^+$ T cells (Figure 4C) and a high level in Tregs (Figure 4B), while $Prf1^{KO}$ mice exhibited a dramatic increase in phosphoSTAT5 in $CD8^+$ T cells and a concomitant decrease in Tregs (Figure 4B, C). $Prf1^{KO}CD8^{\Delta CD25}$ mice showed an almost complete rescue of this IL-2 consumption rewiring, with phospho-STAT5 patterns recapitulating the wildtype situation (Figure 4C, D). Notably, this system did not completely eliminate $CD8^+$ T cell access to IL-2 signaling, with phospho-STAT5 levels marginally higher than wildtype mice (Figure 4C), rather it just corrected the exuberant rewiring occurring in $Prf1^{KO}$ mice. We previously hypothesis that this “IL-2 theft” was responsible for the observed reduction in Treg numbers [21], our results here formally demonstrate this, with an increase of IL-2 availability in the serum (Figure 4E) and a rescue of Treg numbers in $Prf1^{KO}CD8^{\Delta CD25}$ mice (Figure 4B). In addition, while evaluating the presence of soluble CD25 (sCD25), a hallmark diagnostic marker of HLH, we found that $Prf1^{KO}CD8^{\Delta CD25}$ mice presented with very low amounts of sCD25 in their serum, definitively identifying $CD8^+$ T cells as the source of sCD25 during the severe HLH inflammation (Figure 4F). Overall, these data validate the $Prf1^{KO}CD8^{\Delta CD25}$ system for functional testing of the role of $CD8^+$ T cell-mediated IL-2 consumption on the pathogenesis of HLH.

To determine the role of IL-2 consumption on the hematological features of HLH, we infected wildtype, $Prf1^{KO}$ and $Prf1^{KO}CD8^{\Delta CD25}$ mice with LCMV and measured hemoglobin, red cells, hematocrit, reticulocytes and platelets at day 10. Unlike IFN-γ-deficiency, which completely rescued the anemic features of $Prf1^{KO}$ mice (Figure 1), loss of CD25 expression on $CD8^+$ T cells had no effect on any parameter, with hematological

deficiencies equivalent to LCMV-infected *Prf1*$^{KO}$ mice in each case (Figure 5). These results clearly establish the hematological manifestations of HLH as IFN-γ-dependent, CD25-independent.

Despite the severe anemia of *Prf1*$^{KO}$*CD8*$^{\Delta CD25}$ mice following LCMV-infection, the physiological response to infection was markedly improved over *Prf1*$^{KO}$ mice. *Prf1*$^{KO}$*CD8*$^{\Delta CD25}$ mice did not develop the distressed behavior observed in *Prf1*$^{KO}$ mice at day 10 (data not shown), however they experienced the same reduction in weight (Figure 6A). More critically with regards to pathology, the *Prf1*$^{KO}$*CD8*$^{\Delta CD25}$ mice experienced a substantial extension in survival (Figure 6B). This correction of inflammatory pathologies was accompanied by a (at least partial) correction of most of the critical immunological parameters. The CD8$^{+}$ T cell expansion observed in *Prf1*$^{KO}$ mice was largely abrogated (Figure 6C), with the shift towards a TEM and SLEC phenotype intermediate in *Prf1*$^{KO}$*CD8*$^{\Delta CD25}$ mice compared to *Prf1*$^{KO}$ and wildtype mice (Figure 6D, E, F). With the exception of CD69, partial corrections were also observed in PD-1, Ki67 and importantly IFN-γ expression by CD8$^{+}$ T cells (Figure 6G–J). A near complete correction was also observed in the CD4$^{+}$ T cell population, with the shift from naïve to TEM in *Prf1*$^{KO}$ mice effectively quenched by negation of IL-2 consumption by CD8$^{+}$ T cells (Figure 6K). By contrast, neither the liver damage observed in LCMV-infected *Prf1*$^{KO}$ mice (Supplementary Figure 5) nor the cytokine storm (Supplementary Figure 6) were corrected. Together these data demonstrate that escalated CD25 expression, and the resulting “IL-2 theft”, is one of the major mechanistic drivers of the immunological and pathophysiological features of HLH.

## DISCUSSION

Together these data provide a novel, comprehensive model for the pathogenesis of HLH. A disparate group of disease triggers are possible, each of which initiate the upstream events of CD8$^{+}$ T cell hyper-stimulation. In the case of primary HLH, the initiation event is typically an infectious trigger, with defective elimination of infected cells due to impaired cytotoxicity by CD8$^{+}$ T cells and NK cells, and an induced numerical loss of NK cells [21]. This in turn drives excessive antigen-presentation to CD8$^{+}$ T cells [7], likely due to a combination of elevated viral titers and prolonged antigen stimulation (defective elimination of antigen presentation cells) [12]. In secondary HLH, the initiation trigger varies, but regardless results in hyper-stimulation of CD8$^{+}$ T cells against viral, tumor or self-antigens [1,5,8]. The CD8$^{+}$ T cell hyper-stimulation leads to excessive activation and proliferation of CD8$^{+}$ T cells, creating a hyper-activated state [11]. The downstream events directly proximal to pathology here diverge: excessive production of IFN-γ leads to the hematological features, while excessive consumption of IL-2 contributes to the immunological features and ultimately to death due to severe inflammation. The IFN-γ and CD25 pathogenic pathways act independent of each other, with correction of one pathway leaving the other intact. In the mouse model, CD25-deficiency in CD8$^{+}$ T cells gave a partial recovery of the inflammatory components of HLH, demonstrating that CD25 expression, while central, is complemented by additional inflammatory pathways. The remaining mortality in CD25-deficient HLH mice may be due to these residual inflammatory pathways, or to the pathological consequences of the IFN-γ-dependent hematological components. In a translational context,

this incomplete recovery is consistent with the incomplete response to cyclopsorin A treatment.

This synthesized model paints a more complex picture for the role of IFN-γ in HLH. While studies focusing on the hematological features have found IFN-γ inhibition to be an effective approach [9,13,14], our study reveals that it does not prevent the lethal inflammatory signature of HLH in both patients and mouse models. Indeed, IFN-γ, if anything, exhibited regulatory properties over the inflammatory aspects of disease, with enhanced inflammation following genetic removal of IFN-γ in HLH mice. Rather than acting as an inflammatory mediator, it is therefore likely that the key effects of IFN-γ are hematological. The mechanistic pathway for the anaemia is thought to be macrophage-mediated destruction of red cells in the spleen [35], as observed in HLH models [9,11,13,14]. As we also observed a low reticulocyte count (Figure 5), IFN-γ may also function via disrupting the bone-marrow support of erythroid lineage differentiation [36]. Thus, while the ongoing clinical trials of anti-IFN-γ antibody in HLH patients are likely to reverse anemia, they may not be effective as a monotherapy, with the inflammatory aspects requiring a distinct approach. This adjunct therapy will need to target the consumption of IL-2 by $CD8^+$ T cells, the collapse of Tregs, or the downstream (IFN-γ-independent) inflammatory cascade that drives the immune aspects of the disease. Interestingly, inhibition of universal cytokine receptor signaling JAK pathway has been very recently used with success in the same preclinical model of HLH used here [33,37]. The use of ruxolitinib, a JAK1/JAK2 inhibitor, has been proven to be efficient at controlling $CD8^+$ T cells expansion and dampening the cytokine storm in HLH [33]. While this activity has been attributed to IFN-γ inhibition (and, indeed, hematological correction should be attributed to this function), the inhibitor also strongly impacts on other cytokines, including IL-2 which potentially explains the correction of the inflammatory aspects [33,37]. TNF-α in particular is an interesting candidate responsible for the inflammatory cascade downstream of Treg loss, as early experiments have previously demonstrated a long term survival after infection with LCMV in mice doubly knockout for Perforin and TNFR1 [38], and TNF-α levels are reduced in ruxolitinib-treated mice [33,37]. However, as the TNF-α pathway does not depend on JAK½, it is likely that a complex milieu of other cytokines participate upstream.

Finally, we would note that these results have implications beyond HLH. While primary HLH is caused by a rare and specific set of genetic lesions, the diverse causes of secondary HLH demonstrate these principles to be more generic outcomes of excessive hyper-stimulation of $CD8^+$ T cells. Indeed, the same pathways (IFN-γ production and IL-2 consumption) that drive clinical pathology in the extreme context during HLH appear to operate at a sub-clinical level during “normal” $CD8^+$ activation events. Thus even wildtype mice infected with LCMV exhibit a transient anemia and limited temporal drop in Treg number [39], a feature observed in other strong infection responses [40]. These deleterious outcomes can thus perhaps be considered the tolerable costs of mounting an effective $CD8^+$ T cell response, which only rarely escalate into frank immunopathology.

## Supplementary Material

Refer to Web version on PubMed Central for supplementary material.

## ACKNOWLEDGEMENTS

This work was supported by the VIB Gran Challenges, FWO and IUAP (T-TIME). S.H-B. was supported by an FWO post-doctoral fellowship. We thank Max Mazzone (VIB) for providing CD8-Cre transgenic mice. We thank Jeason Haughton and the animal caretakers at the KUL animalium for care of our mice. The Laboratory of Human Genetics of Infectious Diseases is supported by grants from the St. Giles Foundation, the Jeffrey Modell Foundation, The Rockefeller University Center for Clinical and Translational Science grant number 8UL1TR000043 from the National Center for Research Resources and the National Center for Advancing Sciences (NCATS), the National Institutes of Health, the National Institute of Allergy and Infectious Diseases grant number 5R01AI089970–02, The Rockefeller University, and the European Research Council (ERC), the Integrative Biology of Emerging Infectious Diseases Laboratory of Excellence (ANR-10-LABX-62-IBEID) and the French National Research Agency (ANR) under the “Investments for the future” program (grant number ANR-10-IAHU-01), ANR-GENMSMD (ANR-16-CE17–0005-01).

## Abbreviations used

| | |
|---|---|
| **IFN-γ** | Interferon-gamma |
| **HLH** | Hemophagocytic lymphohistiocytosis |
| **IL-2** | Interleukin 2 |
| **IL-6** | Interleukin 6 |
| **TNF-α** | Tumor necrosis factor alpha |
| **NK cells** | Natural killer cells |
| **EBV** | Epstein Barr virus |
| **CMV** | Cytomegalovirus |
| **allo-HSCT** | allogeneic hematopoietic stem cell transplantation |
| **PRF1** | Perforin |
| **IFNγR1** | Interferon-gamma receptor 1 |
| **PBMC** | peripheral blood mononuclear cells |
| **Treg** | regulatory T cell |
| **LCMV** | lymphocytic choriomeningitis virus |
| **KO** | knockout |
| **SLEC** | short-lived effector cells |
| **MPEC** | memory precursor effector cells |
| **BCG** | Bacille Calmette and Guérin |
| **MSMD** | Mendelian susceptibility to mycobacterial disease |
| **STAT** | Signal transducer and activator of transcription |
| **EMSA** | Electrophoretic mobility shift assay |

| | |
|---|---|
| **ES cells** | embryonic stem cells |
| **JAK** | Janus kinase |

## REFERENCES


1. Janka GE, Lehmberg K. Hemophagocytic syndromes - An update. Blood Rev 2014;28:135–42. [PubMed: 24792320]
2. Jordan MB, Allen CE, Weitzman S, Filipovich AH, McClain KL. How I treat hemophagocytic lymphohistiocytosis. Blood 2011;118:4041–52. [PubMed: 21828139]
3. Janka GE, Lehmberg K. Hemophagocytic lymphohistiocytosis: pathogenesis and treatment. Hematol Am Soc Hematol Educ Progr 2013;2013:605–11.
4. Trottestam H, Horne A, Arico M, Egeler RM, Filipovich AH, Gadner H, et al. Chemoimmunotherapy for hemophagocytic lymphohistiocytosis: long-term results of the HLH-94 treatment protocol. Blood 2011;118:4577–84. [PubMed: 21900192]
5. Allen CE, McClain KL. Pathophysiology and epidemiology of hemophagocytic lymphohistiocytosis. Hematol Am Soc Hematol Educ Progr 2015;2015:177–82.
6. Bergsten E, Horne A, Aricó M, Astigarraga I, Egeler RM, Filipovich AH, et al. Confirmed efficacy of etoposide and dexamethasone in HLH treatment: long-term results of the cooperative HLH-2004 study. Blood 2017;130:2728–38. [PubMed: 28935695]
7. de Saint Basile G, Sepulveda FE, Maschalidi S, Fischer A. Cytotoxic granule secretion by lymphocytes and its link to immune homeostasis. F1000Research 2015;4:930. [PubMed: 26594351]
8. Nikiforow S, Berliner N. The unique aspects of presentation and diagnosis of hemophagocytic lymphohistiocytosis in adults. Hematol Am Soc Hematol Educ Progr 2015;2015:183–9.
9. Zoller EE, Lykens JE, Terrell CE, Aliberti J, Filipovich AH, Henson PM, et al. Hemophagocytosis causes a consumptive anemia of inflammation. J Exp Med 2011;208:1203–14. [PubMed: 21624938]
10. Badovinac VP, Hamilton SE, Harty JT. Viral infection results in massive CD8+ T cell expansion and mortality in vaccinated perforin-deficient mice. Immunity 2003;18:463–74. [PubMed: 12705850]
11. Jordan MB, Hildeman D, Kappler J, Marrack P. An animal model of hemophagocytic lymphohistiocytosis (HLH): CD8+ T cells and interferon gamma are essential for the disorder. Blood 2004;104:735–43. [PubMed: 15069016]
12. Jenkins MR, Rudd-Schmidt J a., Lopez J a., Ramsbottom KM, Mannering SI, Andrews DM, et al. Failed CTL/NK cell killing and cytokine hypersecretion are directly linked through prolonged synapse time. J Exp Med 2015;212:307–17. [PubMed: 25732304]
13. Schmid JP, Ho C-H, Chrétien F, Lefebvre JM, Pivert G, Kosco-Vilbois M, et al. Neutralization of IFNγ defeats haemophagocytosis in LCMV-infected perforin- and Rab27a-deficient mice. EMBO Mol Med 2009;1:112–24. [PubMed: 20049711]
14. Binder D, Fehr J, Hengartner H, Zinkernagel RM. Virus-induced transient bone marrow aplasia: major role of interferon-alpha/beta during acute infection with the noncytopathic lymphocytic choriomeningitis virus. J Exp Med 1997
15. Tesi B, Sieni E, Neves C, Romano F, Cetica V, Cordeiro AI, et al. Hemophagocytic lymphohistiocytosis in 2 patients with underlying IFN-γ receptor deficiency. J Allergy Clin Immunol 2015;135:1638–41. [PubMed: 25592983]
16. Staines-Boone AT, Deswarte C, Venegas Montoya E, Sánchez-Sánchez LM, García Campos JA, Muñiz-Ronquillo T, et al. Multifocal Recurrent Osteomyelitis and Hemophagocytic Lymphohistiocytosis in a Boy with Partial Dominant IFN-γR1 Deficiency: Case Report and Review of the Literature. Front Pediatr 2017;5:75. [PubMed: 28516082]
17. Muriel-Vizcaino R, Yamazaki-Nakashimada M, López-Herrera G, Santos-Argumedo L, Ramírez-Alejo N. Hemophagocytic Lymphohistiocytosis as a Complication in Patients with MSMD. J Clin Immunol 2016;36:420–2. [PubMed: 27146670]
18. Avau A, Mitera T, Put S, Put K, Brisse E, Filtjens J, et al. Systemic Juvenile Idiopathic Arthritis-like Syndrome in Mice Following Stimulation of the Immune System With Freund's Complete

Adjuvant: Regulation by Interferon-γ. Arthritis Rheumatol 2014;66:1340–51. [PubMed: 24470407]

19. Canna SW, Wrobel J, Chu N, Kreiger PA, Paessler M, Behrens EM. Interferon-γ mediates anemia but is dispensable for fulminant toll-like receptor 9-induced macrophage activation syndrome and hemophagocytosis in mice. Arthritis Rheum 2013;65:1764–75. [PubMed: 23553372]
20. Sumegi J, Barnes MG, Nestheide SV, Molleran-Lee S, Villanueva J, Zhang K, et al. Gene expression profiling of peripheral blood mononuclear cells from children with active hemophagocytic lymphohistiocytosis. Blood 2011;117:e151–60. [PubMed: 21325597]
21. Humblet-Baron S, Franckaert D, Dooley J, Bornschein S, Cauwe B, Schönefeldt S, et al. IL-2 consumption by highly activated CD8 T cells induces regulatory T-cell dysfunction in patients with hemophagocytic lymphohistiocytosis. J Allergy Clin Immunol, 2016;138:200–2009.e8 [PubMed: 26947179]
22. Jordan Michael, Franco Locatelli Prof, Carl Allen, De Benedetti Fabrizio, Grom Alexei A., Ballabio Maria, Walter Giovanni Ferlin N-0501–04 SG and CDM. A Novel Targeted Approach to the Treatment of Hemophagocytic Lymphohistiocytosis (HLH) with an Anti-Interferon Gamma (IFNγ) Monoclonal Antibody (mAb), NI-0501: First Results from a Pilot Phase 2 Study in Children with Primary HLH. Blood 2015;126 (23).
23. Kägi D, Ledermann B, Bürki K, Seiler P, Odermatt B, Olsen KJ, et al. Cytotoxicity mediated by T cells and natural killer cells is greatly impaired in perforin-deficient mice. Nature 1994;369:31–7. [PubMed: 8164737]
24. Dalton DK, Pitts-Meek S, Keshav S, Figari IS, Bradley A, Stewart TA. Multiple defects of immune cell function in mice with disrupted interferon-gamma genes. Science 1993;259:1739–42. [PubMed: 8456300]
25. Maekawa Y, Minato Y, Ishifune C, Kurihara T, Kitamura A, Kojima H, et al. Notch2 integrates signaling by the transcription factors RBP-J and CREB1 to promote T cell cytotoxicity. Nat Immunol 2008;9:1140–7. [PubMed: 18724371]
26. Rodríguez CI, Buchholz F, Galloway J, Sequerra R, Kasper J, Ayala R, et al. High-efficiency deleter mice show that FLPe is an alternative to Cre-loxP. Nat Genet 2000;25:139–40. [PubMed: 10835623]
27. Utzschneider DT, Legat A, Fuertes Marraco SA, Carrié L, Luescher I, Speiser DE, et al. T cells maintain an exhausted phenotype after antigen withdrawal and population reexpansion. Nat Immunol 2013;14:603–10. [PubMed: 23644506]
28. Battegay M, Cooper S, Althage A, Bänziger J, Hengartner H, Zinkernagel RM. Quantification of lymphocytic choriomeningitis virus with an immunological focus assay in 24- or 96-well plates. J Virol Methods 1991;33:191–8. [PubMed: 1939506]
29. Kong X-F, Vogt G, Chapgier A, Lamaze C, Bustamante J, Prando C, et al. A novel form of cell type-specific partial IFN-gammaR1 deficiency caused by a germ line mutation of the IFNGR1 initiation codon. Hum Mol Genet 2010;19:434–44. [PubMed: 19880857]
30. Oleaga-Quintas C, Deswarte C, Moncada-Vélez M, Metin A, Krishna Rao I, Kanlık-Yüksek S, et al. A purely quantitative form of partial recessive IFN-γR2 deficiency caused by mutations of the initiation or second codon. Hum Mol Genet 2018
31. Brayton CF, Treuting PM, Ward JM. Pathobiology of Aging Mice and GEM. Vet Pathol 2012;49:85–105. [PubMed: 22215684]
32. Shackelford C, Long G, Wolf J, Okerberg C, Herbert R. Qualitative and quantitative analysis of nonneoplastic lesions in toxicology studies. Toxicol Pathol 2002;30:93–6. [PubMed: 11890482]
33. Das R, Guan P, Sprague L, Verbist K, Tedrick P, An QA, et al. Janus kinase inhibition lessens inflammation and ameliorates disease in murine models of hemophagocytic lymphohistiocytosis. Blood 2016;127:1666–75. [PubMed: 26825707]
34. Bustamante J, Boisson-Dupuis S, Abel L, Casanova J-L. Mendelian susceptibility to mycobacterial disease: genetic, immunological, and clinical features of inborn errors of IFN-γ immunity. Semin Immunol 2014;26:454–70. [PubMed: 25453225]
35. Libregts SF, Gutierrez L, de Bruin AM, Wensveen FM, Papadopoulos P, van Ijcken W, et al. Chronic IFN- production in mice induces anemia by reducing erythrocyte life span and inhibiting erythropoiesis through an IRF-1/PU.1 axis. Blood 2011;118:2578–88. [PubMed: 21725055]

36. Goedhart M, Cornelissen AS, Kuijk C, Geerman S, Kleijer M, van Buul JD, et al. Interferon-Gamma Impairs Maintenance and Alters Hematopoietic Support of Bone Marrow Mesenchymal Stromal Cells. Stem Cells Dev 2018;27:579–89. [PubMed: 29649408]

37. Maschalidi S, Sepulveda FE, Garrigue A, Fischer A, de Saint Basile G. Therapeutic effect of JAK½ blockade on the manifestations of hemophagocytic lymphohistiocytosis in mice. Blood 2016;128:60–71. [PubMed: 27222478]

38. Binder D, van den Broek MF, Kägi D, Bluethmann H, Fehr J, Hengartner H, et al. Aplastic anemia rescued by exhaustion of cytokine-secreting CD8+ T cells in persistent infection with lymphocytic choriomeningitis virus. J Exp Med 1998;187:1903–20. [PubMed: 9607930]

39. Srivastava S, Koch MA, Pepper M, Campbell DJ. Type I interferons directly inhibit regulatory T cells to allow optimal antiviral T cell responses during acute LCMV infection. J Exp Med 2014;211:961–74. [PubMed: 24711580]

40. Oldenhove G, Bouladoux N, Wohlfert EA, Hall JA, Chou D, Dos Santos L, et al. Decrease of Foxp3+ Treg cell number and acquisition of effector cell phenotype during lethal infection. Immunity 2009;31:772–86. [PubMed: 19896394]

**Key messages**

- In HLH, hematological features are strictly dependent of IFN-γ. However, in both patient and mouse model, absence of IFN-γ signaling does not prevent inflammatory aspect of the disease.
- IL-2 signaling plays a key role in the excessive $CD8^+$ T cell activation during HLH inflammation, providing potential therapeutic target for HLH treatment.

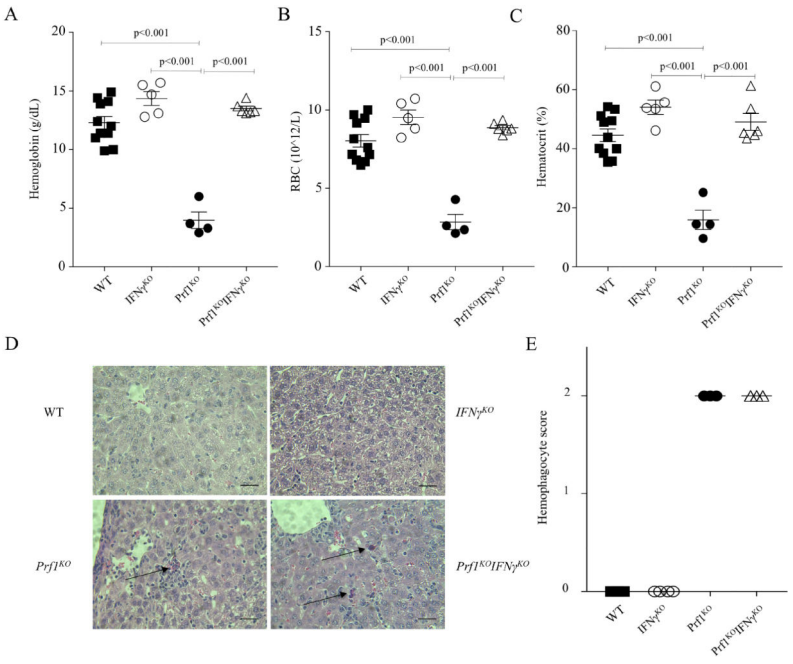


**Figure 1. Hematological component of murine HLH is dependent on excessive IFN-γ production.**

Wildtype mice, *IFN-γ*$^{KO}$, *Prf1*$^{KO}$, and *Prf1*$^{KO}$*IFN-γ*$^{KO}$ mice were infected with LCMV Armstrong. On day 10, blood samples from each strain were assessed for **(A)** hemoglobin **(B)** red blood cells and **(C)** hematocrit (A-C: n=11,5,4, 6). Results pooled from 4 experiments. **(C)** Representative histology from the liver and **(D)** histological scoring for hemophagocyte presence in liver on H&E sections on day 10 (n=3,4,3,3). Arrows indicate hemophagocytes. Scale bar is 50 μm. Analyzed with one-way ANOVA with Tuckey's multiple comparisons test, SEM and individual data points shown.

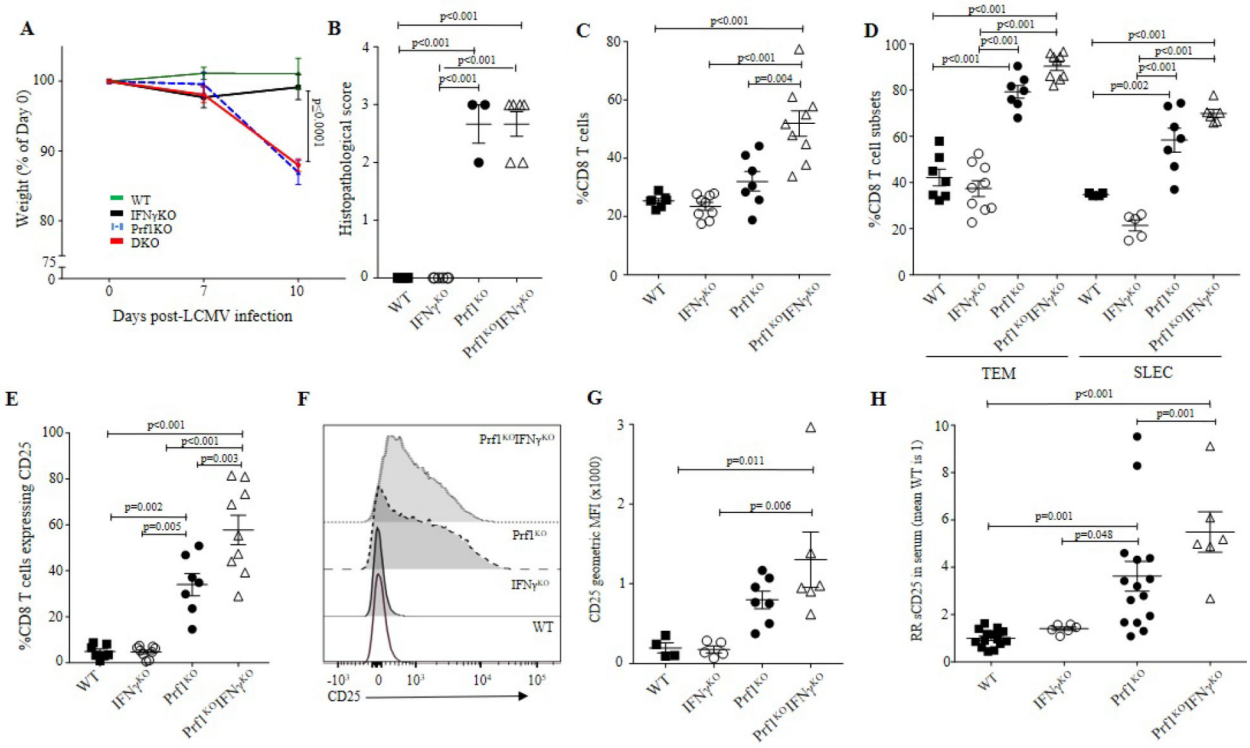


**Figure 2. Inflammatory and physiological aspects of murine HLH arise independent of IFN-γ.**

Wildtype mice, *IFN-γ$^{KO}$*, *Prf1$^{KO}$*, and *Prf1$^{KO}$IFN-γ$^{KO}$* mice were infected with LCMV Armstrong. **(A)** Mouse weights on days 0, 7 and 10 after LCMV infection (n=7,9,7,9). **(B)** Histological scoring for immune cell infiltrates in liver on H&E sections on day 10 (n=5,6,3,6). **(C)** Percentage of CD8+ T cells in the lymph nodes (n=7,9,7,9). **(D)** Percentage of $CD8^+$ T cells in the $CD8^+CD62L^-CD44^+$ effector memory (TEM) (n=7,9,7,9) and percentage of activated $CD8^+$ T cells in the $CD8^+CD127^+KLRG1^{high}$ (SLEC) subsets (n=4,5,7,6). **(E)** Percentage of $CD8^+$ T cells expressing $CD25^+$ (n=7,9,7,9). **(F)** Representative CD25 staining on $CD8^+$ T cells. **(G)** CD25 geometric MFI on total $CD8^+$ T cells (n=4,5,7,6). **(H)** Relative ratio of sCD25 in the serum (n=14,6,15,6). Analyzed with one-way ANOVA with Tuckey's multiple comparisons test, SEM and individual data points shown. Results pooled from 4 experiments and 3 experiments for sCD25 measurements.

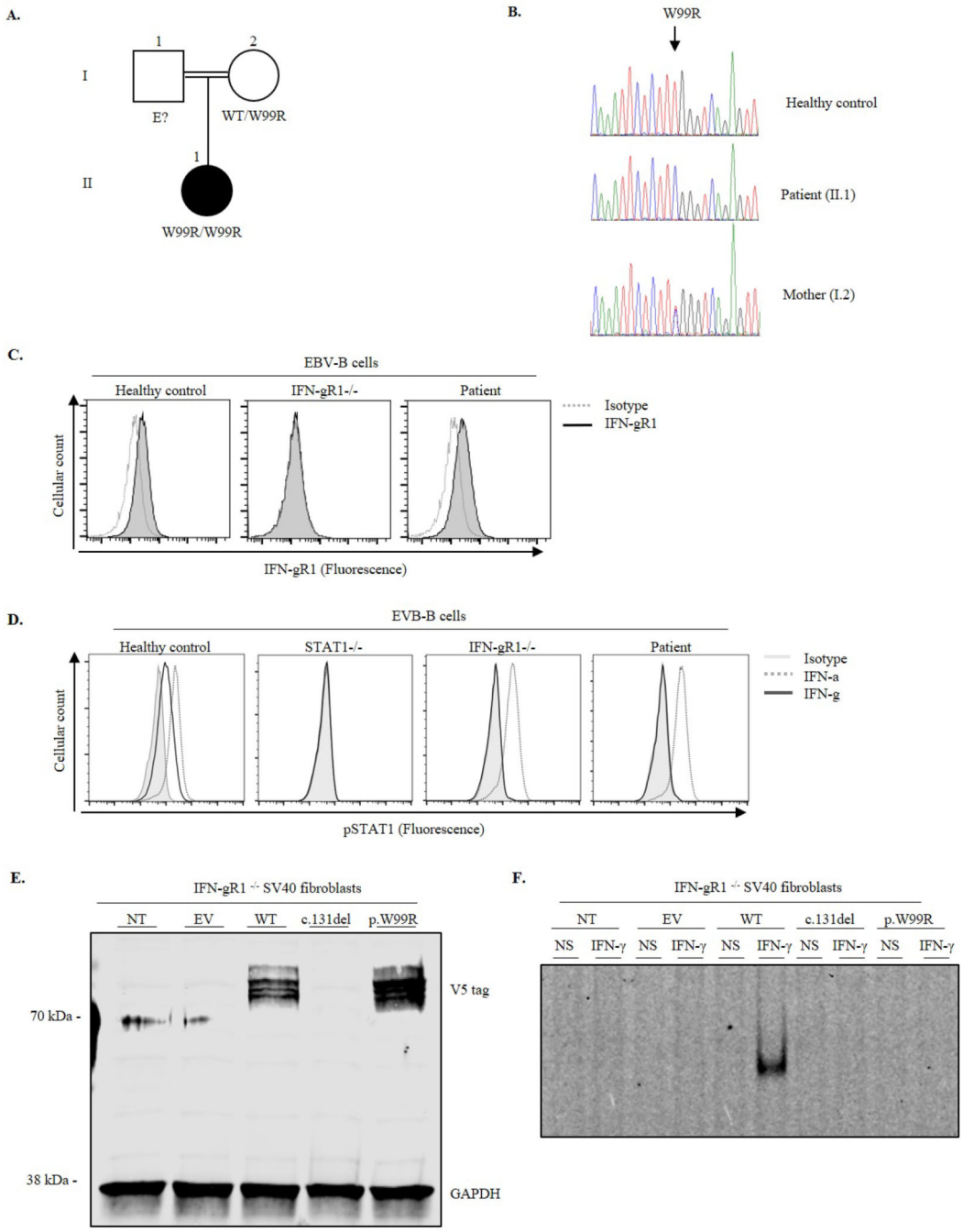


**Figure 3. IFN-γR1 deficiency in a HLH-like patient.**

**(A)** Pedigree of kindred, showing the index case and parents; each generation is designated by a Roman numeral (I-II). No gDNA was available for testing for father labeled “E?”. **(B)** Electropherogram (healthy control, patient (II,1) and her mother) showing the position of the mutation in the IFNGR1 gene. **(C)** Flow cytometry analysis of IFN-γR1 expression on the surface of EBV-B cells from healthy control, IFN-γR1 deficient patient and patient (II,1) with the recessive W99R mutation. The histograms represent the expression of IFN-γR1 (gray filled) and the isotype control (dashed line). **(D)** Phospho-STAT1 response of EBV-B

cells to IFN-γ (black line) or IFN-α (dashed line) stimulation in healthy control, IFN-γR1 deficient patient and patient (II,1). **(E)** IFN-γR1$^{-/-}$ SV40 fibroblasts were left untransfected (NT) or were transiently transfected with EV, WT, c.131del (negative control) o p.W99R mutant- IFNGR1 plasmids. Total lysis and western blots were performed with anti-V5 antibody, with GAPDH as the loading control. **(F)** IFN-γR1$^{-/-}$ SV40 fibroblasts were left untransfected (NT) or were transiently transfected with empty plasmid (EV), wild type (WT), c.131del (negative control) and p.W99R mutant-*IFNGR1* plasmids, and were either left non-stimulated (NS) or stimulated with $10^5$ IU/ml IFN-γ (IFN-γ). DNA-binding activity was then analyzed by EMSA with a GAS probe.

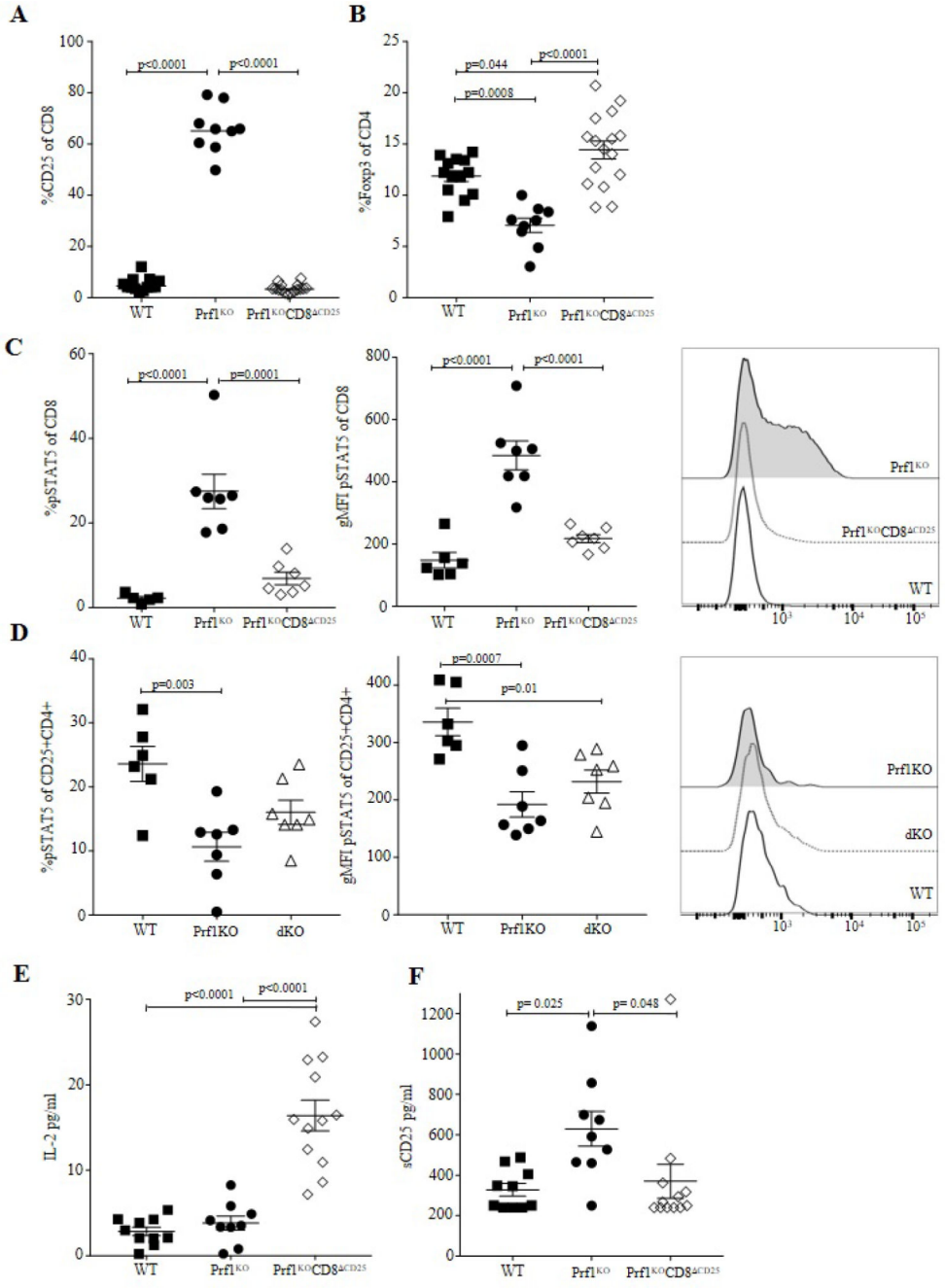


**Figure 4. Removal of CD25 expression on CD8+ T cells prevents rewiring of IL-2 consumption and the collapse of Tregs during HLH.**

Wildtype mice, *Prf1*$^{KO}$, *Prf1*$^{KO}$*CD8*$^{\Delta CD25}$ mice were infected with LCMV Armstrong, and assessed on day 10. **(A)** Percentage of CD8$^{+}$ T cells expressing CD25 (n=13,9,16). **(B)** Percentage of Treg within the CD4$^{+}$ T cell population (n=13,9,16). **(C)** (left) Percentage of cells positive for phospho-STAT5 staining in CD8$^{+}$ T cells, (middle) geometric MFI for phospho-STAT5 staining on CD8$^{+}$, (right) representative phospho-STAT5 staining on CD8$^{+}$ T cells (n=5,7,7). **(D)** (left) Percentage cells positive for phospho-STAT5 staining in CD4$^{+}$CD25$^{+}$ Treg cells within the CD4$^{+}$ T cell population, (middle) geometric MFI of

phospho-STAT5 staining on $CD4^+CD25^+$ Treg cells and (right) representative phospho-STAT5 staining on $CD4^+Foxp3^+$ Treg cells (n=6,7,7). **(E)** IL-2 concentration in the serum (n=10,9,12). **(F)** Soluble CD25 in the serum (n=10,9,12). Analyzed with one-way ANOVA with Tuckey's multiple comparisons test, SEM and individual data points shown. Results pooled from 4 experiments and 3 experiments for phospho-STAT5 measurements.

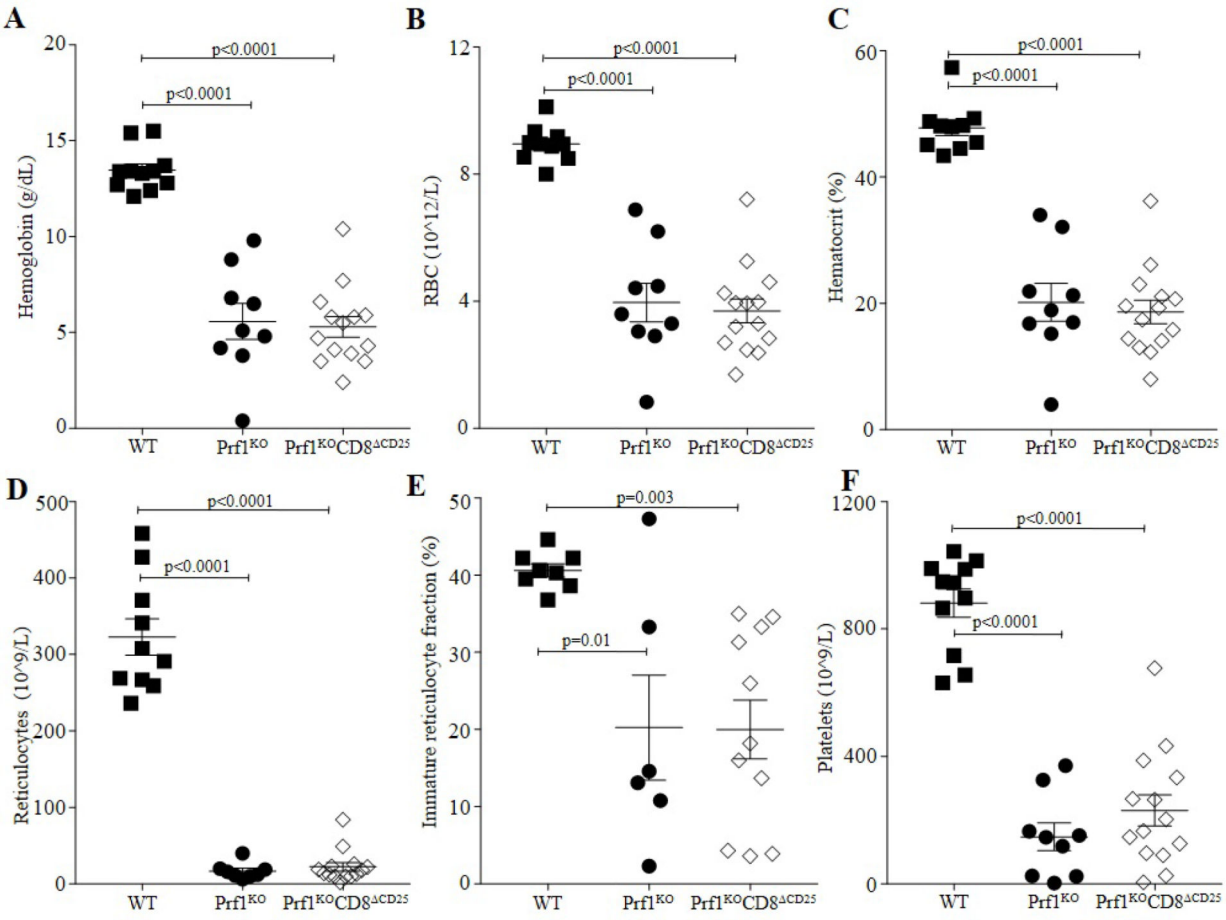


**Figure 5. Correction of the IL-2 consumption phenotype of hyper-activated CD8+T cells does not impact the hematological features of HLH.**

Wildtype mice, *Prf1*$^{KO}$, *Prf1*$^{KO}$*CD8*$^{\Delta CD25}$ mice were infected with LCMV Armstrong. On day 10, blood samples from each strain were assessed for **(A)** hemoglobin (n=11, 9, 14), **(B)** red blood cells (n=10, 9, 14), **(C)** hematocrit (n=11, 9, 14) **(D)** reticulocytes (n=10, 8, 14), **(E)** immature reticulocyte fraction (IRF) (n=8, 6, 11) and **(F)** platelets (n=11, 9, 14). Analyzed with one-way ANOVA with Tuckey's multiple comparisons test, SEM and individual data points shown. Results pooled from 4 experiments.

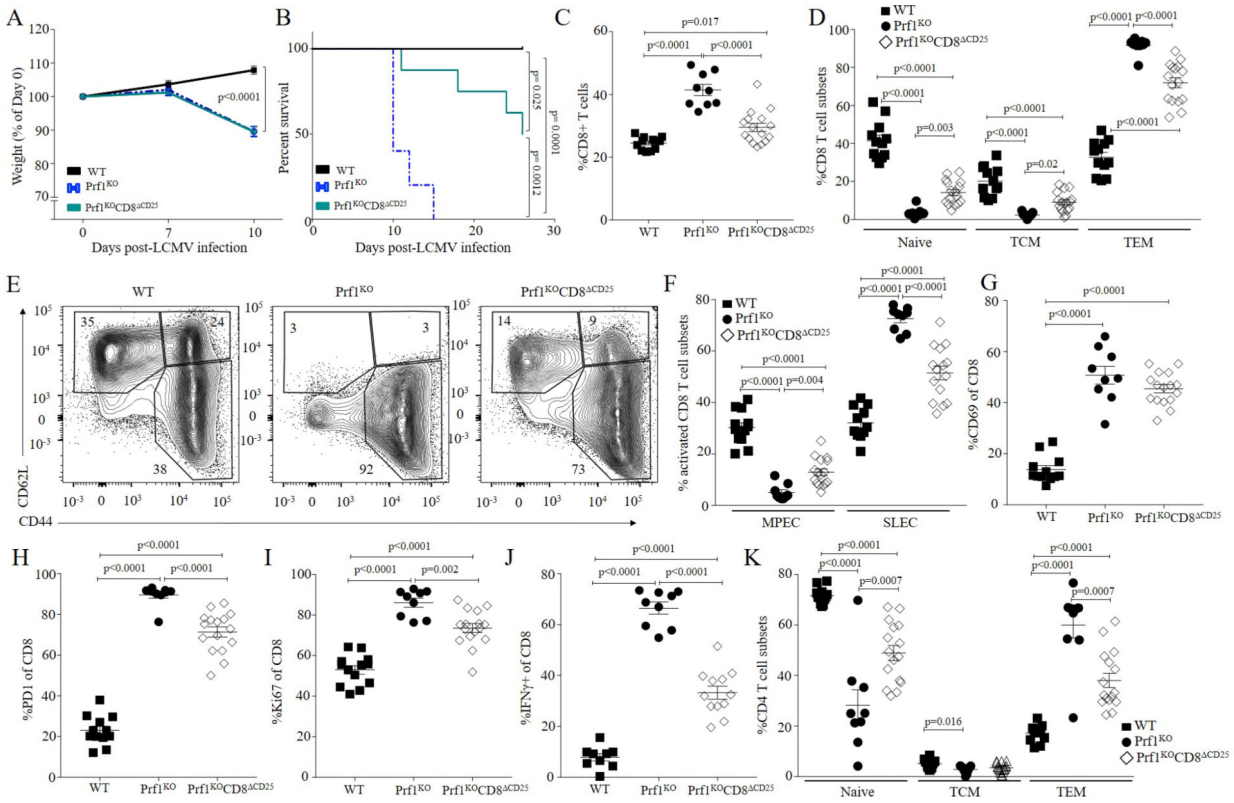


**Figure 6. Immunological and pathophysiological processes of HLH are dependent on CD25 expression by CD8$^+$ T cells.**

Wildtype mice, *Prf1$^{KO}$*, *Prf1$^{KO}$CD8$^{\Delta CD25}$* mice were infected with LCMV Armstrong, and assessed for immunological features on day 10. **(A)** Mouse weights on days 0, 7 and 10 after LCMV infection (n=10,7,13). **(B)** Survival following LCMV infection (n=8,5,8). **(C)** Percentage of CD8$^+$ T cells in the lymph nodes(n=12,9,16). **(D)** Percentage and **(E)** representative flow cytometry for CD8$^+$ T cells in the naïve (CD62L$^+$CD44$^-$), central memory (TCM; CD62L$^+$CD44$^+$), and effector memory (TEM; CD62L$^-$CD44$^+$) class (n=12,9,16). **(F)** Percentage of activated CD8$^+$ T cells in the CD8$^+$CD127$^+$KLRG1$^{low}$ (MPEC) (n=12,9,16) and CD8$^+$CD127$^-$KLRG1$^{high}$ (SLEC) subsets (n=11,9,15). **(G)** Percentage of CD8$^+$ T cells expressing CD69 (n=12,9,16), **(H)** PD-1 (n=12,9,16), **(I)** Ki67 (n=13,9,16) and **(J)** IFN-γ (n=9,9,12). **(K)** Percentage of CD4$^+$ T cells in the naïve (CD62L$^+$CD44$^-$), central memory (TCM; CD62L$^+$CD44$^+$), and effector memory (TEM; CD62L$^-$CD44$^+$) class (n=12,9,16). Analyzed with one-way ANOVA with Tuckey's multiple comparisons test, SEM and individual data points shown. Results pooled from 3 to 4 experiments.